Korean J. Chem. Eng., **24**(1), 154-164 (2007)

Numerical simulation on silane plasma chemistry in pulsed plasma process to prepare a-Si : H thin films

Dong-Joo Kim, Jin-Yi Kang, Anna Nasonova, Kyo-Seon Kim† and Sang-June Choi*

Department of Chemical Engineering, Kangwon National University, Chuncheon, Gangwon-do 200-701, Korea
*Department of Environmental Engineering, KyungPook National University,
1370 Sankyuk-dong, Buk-gu, Daegu 702-701, Korea
(*Received 1 June 2006 • accepted 21 September 2006*)

Abstract−We numerically calculated the effects of pulse modulation (plasma-on and -off times) on the concentration changes of the chemical species (SiH_4, SiH_x, SiH_x^+ and polymerized negative ions) and also the growth rate of a-Si : H thin films in the pulsed SiH_4 plasmas. During the plasma-on, SiH_x is generated quickly by a fast dissociative reaction of SiH_4, but, during plasma-off, SiH_x disappears rapidly by a reaction with hydrogen and also by the deposition onto the reactor wall. During the plasma-on, the negative ions are polymerized by the reactions with SiH_4, but, during the plasma-off, they disappear by neutralization reactions with positive ions. As the plasma-on time increases or as the plasma-off time decreases, the time-averaged concentrations of SiH_x and negative ions and also the time-averaged film growth rate increase. This study shows quantitatively that polymerized negative ions, which are not considered to be preferred precursors for the high-quality thin films, can be efficiently reduced by the pulsed plasma process.

Key words: Pulse Modulation, SiH_4 Plasma Chemical Reactions, Pulsed Plasmas, Polymerization of Negative Ions, High-quality Thin Film

INTRODUCTION

Hydrogenated amorphous silicon (a-Si : H) thin films are widely used as solar cells, image sensors, electrophotographic drums, and thin film transistors and are usually prepared by SiH_4 plasma chemical vapor deposition (PCVD). Recently, the deposition of particles in the size range from a few nm's to microns generated in the plasmas results in the deterioration of the quality of a-Si : H thin films [Fukuzawa et al., 1999; Kim and Kim, 2000; 2002a, b; Kim et al., 2003a, b, c; Koga et al., 2002, 2004; Shiratani et al., 1999; Watanabe et al., 2002]. The SiH_4 PCVD processes are operated in the condition of low SiH_4 partial pressure to reduce the generation and growth of particles at the cost of decrease in the deposition rate [Madan et al., 1999; Madan and Morrison, 1998; Maemura et al., 1999]. To deposit the a-Si : H thin film economically and efficiently by using the plasma processes, it is desirable to increase the deposition rate without the generation and growth of particles and/or the deposition of nanosized cluster particles.

There are several studies on the suppression of the generation and growth of particles in the SiH_4 plasma reactor for preparing a-Si : H thin films by using the pulse modulation or the thermophoretic force due to temperature gradient or by adjusting the gas flow pattern or the distance between the powered and ground electrodes [Fukuzawa et al., 1999; Itagaki et al., 2000; Kim and Kim, 2000, 2002a; Kim et al., 2003a, b; Kirimura et al., 1994; Koga et al., 2002, 2004; Madan et al., 1999; Madan and Morrison, 1998; Maemura et al., 1999; Shiratani et al., 1999; Watanabe et al., 2002]. Watanabe and his colleagues [Fukuzawa et al., 1999; Koga et al., 2004; Shiratani et al., 1999] suggested that the growth of nanosized particles in the plasma reactor can be suppressed efficiently by using the pulse-modulated plasma technique. They also developed the cluster-suppressed plasma method by heating the electrodes and also by removing the stagnation zone by changing the gas flow pattern inside the plasma reactor, and they successfully prepared the high-quality thin films of a-Si : H [Koga et al., 2002; Watanabe et al., 2002]. Kirimura et al. [1994] investigated the effects of the plasma parameter changes on the particle growth and on the properties of a-Si : H thin films in the pulsed plasma process, and they synthesized the a-Si : H films of high-quality at a high deposition rate by the amplitude modulated plasmas. Maemura et al. [1999] reported that the particle generation can be controlled by changing the electrode distance with heating the electrodes in the SiH_4 PCVD reactor, and they prepared the a-Si : H films with a good opto-electronic property even at a high deposition rate. Madan and Morrison [1998] reported that the amorphous/polycrystalline silicon thin films were synthesized at the maximum deposition rate of 1.5 nm/s in the pulse-modulated PCVD. Itagaki et al. [2000] used the pulsed electron cyclotron resonance plasmas to synthesize the a-Si : H thin films, and showed that the deposition rate and the quality of thin films could be changed by pulse modulation. The high-quality thin films then can also be grown at a deposition rate of 1.4 nm/s without substrate heating.

Economou and his colleagues [Midha and Economou, 2000; Ramamurthi and Economou, 2002' studied the evolution of chemical species in the pulsed Cl_2 PCVD process numerically by using the fluid approach method. They addressed the effects of the process variables on the spatio-temporal evolutions of chemical concentrations, and showed that the transition of the electron-dominated plasmas to the ion-ion plasmas. The modulation of negative ion concentrations during the plasma-on (t_{on}) and -off (t_{off}) times then depends on the changes in the process variables. Meyyappan [1996]

---

†To whom correspondence should be addressed.
E-mail: kkyoseon@kangwon.ac.kr

analyzed the pulse-time modulated high density Cl_2 and CF_4 plasmas for etching and deposition processes by using a spatially averaged model, and showed that the duty ratio and pulse frequency affect the plasma density in the plasmas and that the processing rate and etch selectivity can be improved by using the pulse-time modulated discharges. Ashida and Lieberman [1997] used a spatially averaged model to simulate the pulse-power modulated high density Cl_2 plasmas, and reported that the electronegativity of the plasmas is significantly affected by the recombination coefficient of the Cl atoms on the wall and that negative ions can be efficiently extracted from the bulk plasmas by a longer t_{off} than 10's ms. Kim and Kim [2005] showed the dynamics of concentrations of chemical species, which might be important for the evolution of negative ions, as a function of time during plasma-on and -off, assuming that the particles in plasma processes can be formed homogeneously from the polymerized negative ions.

In this study, we numerically investigated the effects of pulse modulation (t_{on} and t_{off}) on the plasma chemistry, film growth rate, and cluster generation in the pulsed SiH_4 plasmas. We analyzed the effects of the plasma chemical reactions, fluid convection, electrical migration, diffusion, and deposition on the electrodes and reactor wall in the model equations for chemical species. We showed the evolutions of several chemical species which are important for film growth and also for particle generation in the pulsed SiH_4 plasmas during t_{on} and t_{off}. We included 36 plasma chemical reactions in the pulsed SiH_4 plasmas, and analyzed the evolutions of chemical species for the processing time of 1 s within a reasonable CPU time by applying a constant concentration and energy of electrons in the plasma reactor.

THEORY

The pulsed plasma reactor proposed by Watanabe and his colleagues [Fukuzawa et al., 1999; Shiratani et al., 1999] as shown in Fig. 1 was applied for this numerical analysis. The upper and lower electrodes in the diameter of 8.5 cm were separated by a distance of 5 cm, and were assumed to have many perforations so that the input and output gas streams could pass through both electrodes. Such a design for electrodes allows us to assume one-dimensional plug flow of the gas stream inside the reactor, and to neglect the momentum balance equation in the model equations.

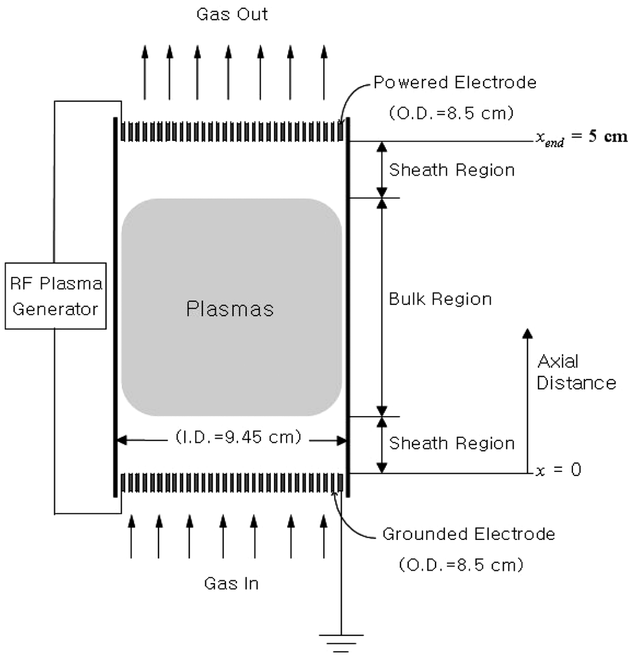

Fig. 1. Schematic of the silane pulsed plasma reactor for modeling.

1. SiH_4 Chemical Reactions in the Pulsed Plasmas

There are more than 50 chemical species and 200 chemical reactions in the SiH_4 plasmas for semiconductor processing [Courteille et al., 1996; Fridman et al., 1996; Howling et al., 1994, 1996; Kushner, 1988]. Howling and his colleagues [Courteille et al., 1996; Howling et al., 1994, 1996] suggested that negative ions can be polymerized homogeneously to form high-mass chemical species in the SiH_4 plasmas on the basis of the experimental observations. We considered 18 chemical species and 36 chemical reactions that might be important for film growth and polymerization of negative ions.

During t_{on}, the neutral molecules (SiH_4) are converted into the reactive radicals (SiH_x), positive (SiH_x^+) and negative (SiH_x^-) ions, and vibrationally excited molecules (SiH_4(v1, 3) and SiH_4(v2, 4)) by the collision with the energetic electrons. The electron impact dissociative reactions, R_1-R_5 of SiH_4, are [Kushner, 1988]:

$$SiH_4+e \rightarrow SiH_x^-(SiH_2^- \text{ or } SiH_3^-)+(H \text{ or } H_2) \quad k_1=4\times10^{-13}\ cm^3s^{-1}, \quad (R_1)$$

$$SiH_4+e \rightarrow SiH_x(\text{neutrals})+(H \text{ or } H_2) \quad k_2=2\times10^{-10}\ cm^3s^{-1}, \quad (R_2)$$

$$SiH_4+e \rightarrow SiH_x^+ +(H \text{ or } H_2) \quad k_3=1.43\times10^{-11}\ cm^3s^{-1} \quad (R_3)$$

$$SiH_4+e \rightarrow SiH_4(v2, 4)+e \quad k_4=8.34\times10^{-9}\ cm^3s^{-1}, \quad (R_4)$$

$$SiH_4+e \rightarrow SiH_4(v1, 3)+e \quad k_5=8.74\times10^{-9}\ cm^3s^{-1}. \quad (R_5)$$

There are two radicals mainly produced by the electron impact dissociative reactions with SiH_4 : SiH_3, the precursors for a-Si : H thin films in SiH_4 plasmas, and SiH_2, the precursors for the polymerized neutral clusters. According to the theoretical study of Bhandarkar et al. [2000], the SiH_2 radical insertion can be important in the production of small clusters, Si_nH_x (n~3 or 4), even though the model results were overestimated in comparison with the experiments due to the large reaction rates of SiH_2 insertion. In our study, we solved the governing equation for SiH_x instead of SiH_2 and SiH_3, respectively, to reduce a computational time. The reaction rate constants of SiH_4 with H and of SiH_3 recombination are smaller than that of SiH_4 with electrons (R_2) by the order of 100 and 10, respectively, according to Kushner [1988]. Thus, we did not include the reaction of SiH_4 with H for SiH_3 production and of SiH_3 recombination with SiH_3 for SiH_2 production in our study. The vibrationally excited molecules are relaxed by the collisions with hydrogen as follows [Kushner, 1988]:

$$SiH_4(v2, 4)+H_2 \rightarrow SiH_4+H_2 \quad k_6=3.05\times10^{-12}\ cm^3s^{-1}, \quad (R_6)$$

$$SiH_4(v1, 3)+H_2 \rightarrow SiH_4+H_2 \quad k_7=6.08\times10^{-11}\ cm^3s^{-1}. \quad (R_7)$$

SiH_x can also be formed by a recombination reaction (R_8) between positive ions and electrons, and is consumed by electron attachment (R_9) and hydrogen adsorption (R_{10}) reactions [Kushner, 1988].

$$SiH_x^+ +e \rightarrow SiH_x(\text{neutrals})+H \quad k_8=3.38\times10^{-7}\ cm^3s^{-1}, \quad (R_8)$$

$$SiH_x+e \rightarrow SiH_x^- \qquad k_9=4\times10^{-13}\ cm^3s^{-1}, \qquad (R_9)$$

$$SiH_x+H_2 \rightarrow SiH_4(or +H) \qquad k_{10}=1\times10^{-12}\ cm^3s^{-1}. \qquad (R_{10})$$

Positive ions disappear by a recombination reaction with electrons (R_8) and neutralization reactions with negative ions (R_{11}-R_{23}) [Kushner, 1988].

$$SiH_x^+ +Si_nH_x^- \rightarrow Si_{n+1}H_{x'}+(H\ or\ H_2) \qquad (n=1\text{-}13) \qquad (R_{11}\text{-}R_{23})$$

($k_{(10+n)}$, n=1, 5×10^{-7} cm^3s^{-1}, n=2, 1.25×10^{-7} cm^3s^{-1}, n=3, 1.4×10^{-7} cm^3s^{-1}, n=4, 1.6×10^{-7} cm^3s^{-1}, n=5, 1.8×10^{-7} cm^3s^{-1}, n=6-13, 2×10^{-7} cm^3s^{-1}).

There are several reports on possible precursors (mainly negative ions and radicals) for the formation of high-massed cluster particles which are negatively charged in the plasma reactor [Courteille et al., 1996; Fukuzawa et al., 1999; Howling et al., 1994, 1996; Shiratani et al., 1999]. Fridman et al. [1996] proposed that the negative ions can be polymerized by the reactions with the vibrationally excited molecules (SiH_4(v1, 3) and SiH_4(v2, 4)). Howling and his colleagues [Howling et al., 1994, 1996; Shiratani et al., 1999] proposed that negative ions are polymerized to the higher mass-clusters by the polymerization reactions with SiH_4 (R_{24}-R_{36}) and can grow in the plasma reactor. They assumed that the polymerization reactions (R_{24}-R_{36}) of negative ions are pseudo-first order with respect to negative ions and are independent of the SiH_4 concentration, and measured the rate constants, k_{24}-k_{36}, for those reactions with the unit of s^{-1} [Howling et al., 1994, 1996; Shiratani et al., 1999].

$$Si_nH_x^- +SiH_4 \rightarrow Si_{n+1}H_{x'}^- +(H\ or\ H_2) \qquad (n=1\text{-}13) \qquad (R_{24}\text{-}R_{36})$$

($k_{(23+n)}$, n=1, 10^4 s^{-1}, n=2, 2.5×10^3 s^{-1}, n=3, 2.8×10^3 s^{-1}, n=4, 3.2×10^3 s^{-1}, n=5, 3.6×10^3 s^{-1}, n=6-13, 4×10^3 s^{-1}).

Many neutral clusters, Si_nH_x, can be produced in a plasma reactor and are charged negatively by the electron attachment during the discharge [Fridman et al., 1996; Nomura et al., 1996]. Recently, Gallagher et al. [2002] reported that the electron attachment to Si_2H_n during the discharge can play a role to produce SiH_x^-. We neglected the electron attachment reactions to Si_nH_x in our study because the rate constants of R_{24}-R_{36} for the growth of negative ions are the empirical data including the electron attachment reactions to Si_nH_x. In this study, the SiH_4 concentration changes according to the reactor length with time. The reaction rates of R_{24}-R_{36} were modified as the second order reactions with respect to negative ions and SiH_4 to account for the changes in SiH_4 concentration in the reactor.

Just after t_{off}, the electrons disappear rapidly by ambipolar diffusion with SiH_x^+ and a recombination on the wall, or the electron attachment to the neutrals within 10's μs [Ashida and Lieberman, 1997; Courteille et al., 1996; Fridman et al., 1996; Howling et al., 1994, 1996; Kushner, 1988; Meyyappan, 1996; Midha and Economou, 2000; Ramamurthi and Economou, 2002]. The reactions involved with the electrons are considered only during t_{on}, while the reactions involved with the molecules and radicals are considered during both t_{on} and t_{off}. There will be several reaction paths for the polymerization of negative ions in the SiH_4 plasmas, but the rate constants of the polymerization reactions (R_{24}-R_{36}) were obtained empirically for the continuous-wave plasma discharge by assuming that the polymerization reactions of negative ions ($Si_nH_{x'}^-$) with SiH_4 are dominant [Courteille et al., 1996; Howling et al., 1994, 1996]; therefore, we considered those polymerization reactions only during t_{on}.

2. Governing Equations for Chemical Species in the Pulsed Plasmas

In the plasma reactor, the electron concentration depends on the position and time, and we should use kinetic approaches on the basis of the particle-in-cell/Monte Carlo simulation or the hybrid Monte Carlo/fluid model to predict the exact electron concentration [Graves, 1987; Graves and Jensen, 1986; Kushner, 1988; Midha and Economou, 2000; Ramamurthi and Economou, 2002; Sato and Tagashira, 1991]. But we did not solve the governing equation for electrons to reduce the computational time, and had assumed that the electron number concentration and the electron energy during t_{on} were uniform inside the reactor. We used the time-averaged electric field strength in the plasma reactor, which changed as a function of position but not as a function of time [Kim and Ikegawa, 1996; Kim and Kim, 1997, 2000; Sato and Tagashira, 1991]. The fluid approach method is known to be numerically effective in terms of the CPU time and we developed the model equations for chemical species to analyze the plasma chemistry in the SiH_4 pulsed plasma processes on the basis of the fluid approach.

The number concentration (N_i) for chemical species, i, is balanced with the effects of plasma chemical reactions, convection, diffusion, electrical migration and deposition onto the electrodes and reactor wall, and the governing equations for N_i's in the pulsed plasma reactor are expressed as follows [Kim and Ikegawa, 1996; Kim and Kim, 1997, 2000]:

$$\frac{\partial N_i}{\partial t}=\sum_{j=1}^{36}\alpha_{ij}(RXN)_j-\nabla(u_sN_i-D_i\nabla N_i-\delta_i\mu_iEN_i)-J_w\left(\frac{2}{R}\right) \qquad (i=1\text{-}18). \qquad (1)$$

In Eq. (1), t, α_{ij} and $(RXN)_j$ are the time, stoichiometric coefficient for i species in the *j*th reaction and rate of the *j*th reaction. u_s is the gas velocity inside the reactor and is assumed to be uniform due to the perforated electrodes. The diffusion coefficients (D_i) for chemical species were calculated by the Chapman and Enskog equation [Reid et al., 1977]. We assumed that the reactor pressure in the plasma reactor was constant and neglected the effect of chemical reactions on the gas flow rate because the chemical species we considered in this model were in low concentration. δ_i is 1 for positive ions, −1 for negative ions and 0 for neutrals. The electric migration coefficient, μ_i, was calculated according to the Einstein relationship [Chen, 1984]. E is the time-averaged electric field as a function of position inside the plasma reactor [Kim and Ikegawa, 1996; Kim and Kim, 1997, 2000; Sato and Tagashira, 1991]. During t_{on}, the E in the bulk plasma region ($x_{pos}\le x\le x_{neg}$) is zero, and the E in the sheath regions ($0\le x\le x_{pos}$, $x_{neg}\le x\le x_{end}$) can be expressed by the Child-Langmuir equation by assuming a collisionless plasma as follows [Kim and Ikegawa, 1996; Kim and Kim, 1997, 2000:

$$E=E_{max}\left[1-\left(\frac{x}{x_{pos}}\right)^{1/3}\right] \qquad \text{for } 0\le x\le x_{pos}, \qquad (2)$$

$$E=0 \qquad \text{for } x_{pos}\le x\le x_{neg}, \qquad (3)$$

$$E=E_{min}\left[1-\left(\frac{x_{end}-x}{x_{end}-x_{neg}}\right)^{1/3}\right] \qquad \text{for } x_{neg}\le x\le x_{end}. \qquad (4)$$

In Eqs. (2)-(4), E_{max} and E_{min} are the maximum and minimum time-averaged electric fields at the powered and the grounded electrodes, respectively. x_{end} is the reactor length, and x_{pos} and x_{neg} are the axial positions where the time-averaged electric field becomes zero near the powered and the grounded electrodes, respectively. During t_{on}, the sheath regions are formed near two electrodes by the differences between the concentrations of positively and negatively charged species, and the thicknesses of the sheath regions (x_{pos} and (x_{end}-x_{neg})) are assumed to be 0.3 cm in this analysis [Sato and Tagashira, 1991]. During t_{off}, the electric field strength between the two electrodes can be set for zero, because the sheath regions disappear quickly within 10's μsec after the plasma discharge stops [Anders, 2004]. It is assumed that the transport phenomena for ionized species for 10's μsec just after t_{on} or t_{off} do not significantly affect the concentration profiles of positive and negative ions in the plasma reactor. The electric fields in the sheath regions follow Eqs. (2)-(4) during t_{on}, but become zero just after t_{off}. J_w is the deposition flux of chemical species onto the reactor wall and we considered the deposition of SiH_x radicals. R is the reactor diameter.

For SiH_4 and SiH_x, we used the Danckwerts boundary conditions at the reactor inlet and outlet [Danckwerts, 1953]. The ions move fast under the electric field in the plasmas. For positive and negative ions, we used the flux boundary conditions at the reactor inlet and outlet during t_{on}, which worked well under the typical discharge condition by Graves et al. [Graves, 1987; Graves and Jensen, 1986], but, during t_{off}, we used the Danckwerts boundary conditions for all charged chemical species at the reactor inlet and outlet. During t_{off}, positive and negative ions can diffuse quickly to the electrodes; therefore, we used 0.15 as the sticking coefficients for both ions at the electrodes. Since SiH_x can diffuse onto the reactor wall during t_{on} and t_{off}, the sticking coefficient of SiH_x was assumed to be 0.15 [Shiratani et al., 1999]. The governing equations for the 18 chemical species (Eqs. (1)-(4)) were solved numerically by using the subroutine VODPK to calculate the concentration profiles for chemical species in the pulsed plasma reactor.

RESULTS AND DISCUSSION

The reactor length (x_{end}), total gas flow rate, reactor pressure and temperature inside the reactor are 5 cm, 20 sccm, 0.1 Torr and 300 K, respectively, and they are the same as the experimental conditions as in Fukuzawa et al. [1999]. The electron concentrations were measured from 4×10^9 to 7×10^9 #/cm^3 in the pulsed SiH_4 plasmas by Fukuzawa et al. [1999]. The electron concentration was assumed to be 5×10^9 #/cm^3 during t_{on}, but zero during t_{off}. E_{max} and E_{min} are 100 and −100 V/cm for the actual electric fields in the industrial PCVD reactor [Graves, 1987; Graves and Jensen, 1986; Kim and Ikegawa, 1996; Sato and Tagashira, 1991]. We considered t_{on} and t_{off} in the range from 10^{-5} to 1.0 s, and the standard conditions for t_{on} and t_{off} were assumed to be 0.01 s and 0.02 s, respectively, in this study.

Fig. 2 shows the evolution of SiH_4 concentration profiles along the axial distance during (a) t_{on} and (b) t_{off}. The SiH_4 concentration at the outlet is lower than at the inlet by the effect of chemical reactions. In Fig. 2(a), during t_{on}, SiH_4 is consumed by the collision with electrons (R_1-R_5), and its concentration decreases with time, but does not reach a steady state condition for the continuous-wave plasmas until t_{on}=0.01 s. In Fig. 2(b), after the plasma discharge stops, the electrons disappear quickly and the SiH_4 disappearance reactions (R_1-R_5) by the electron collisions become zero, and its concentration increases with time toward the initial SiH_4 concentration. In Figs. 3(a, b), the evolution of the SiH_x concentration profiles is illustrated along the axial distance during t_{on} and t_{off}, respectively. In the beginning of the plasma discharge, the SiH_x radicals are generated fast from the SiH_4 dissociation reaction (R_2), and the SiH_x concentration in the plasma reactor increases with time and reaches the

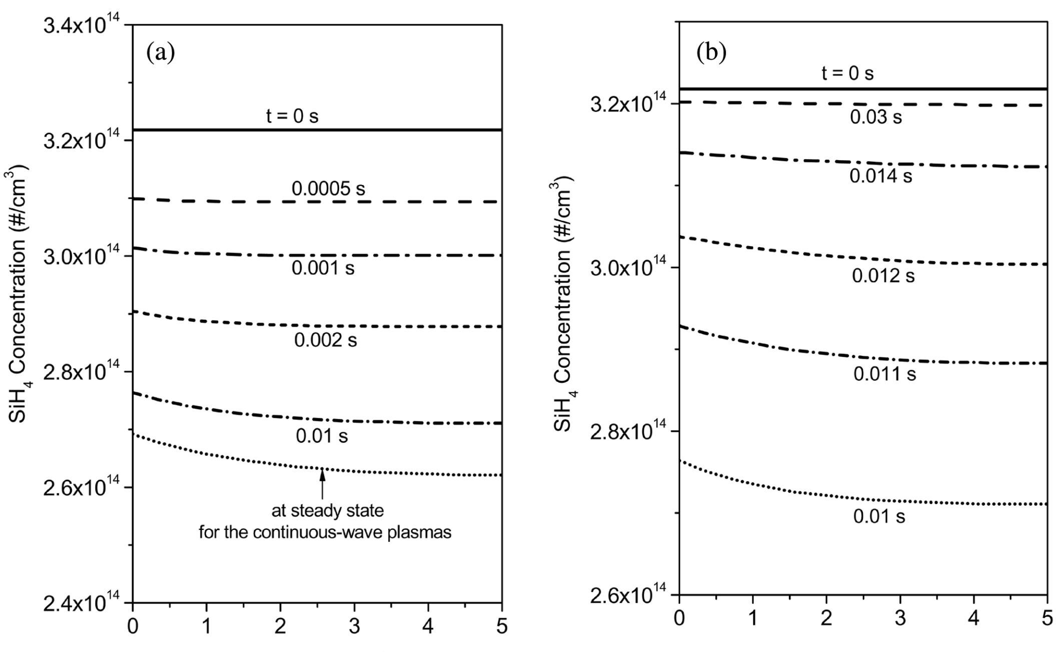

Fig. 2. (a) Evolution of SiH_4 concentration profiles along the axial distance for various times during t_{on} (t_{on}=0.01 s and t_{off}=0.02 s). (b) Evolution of SiH_4 concentration profiles along the axial distance for various times during t_{off} (t_{on}=0.01 s and t_{off}=0.02 s).

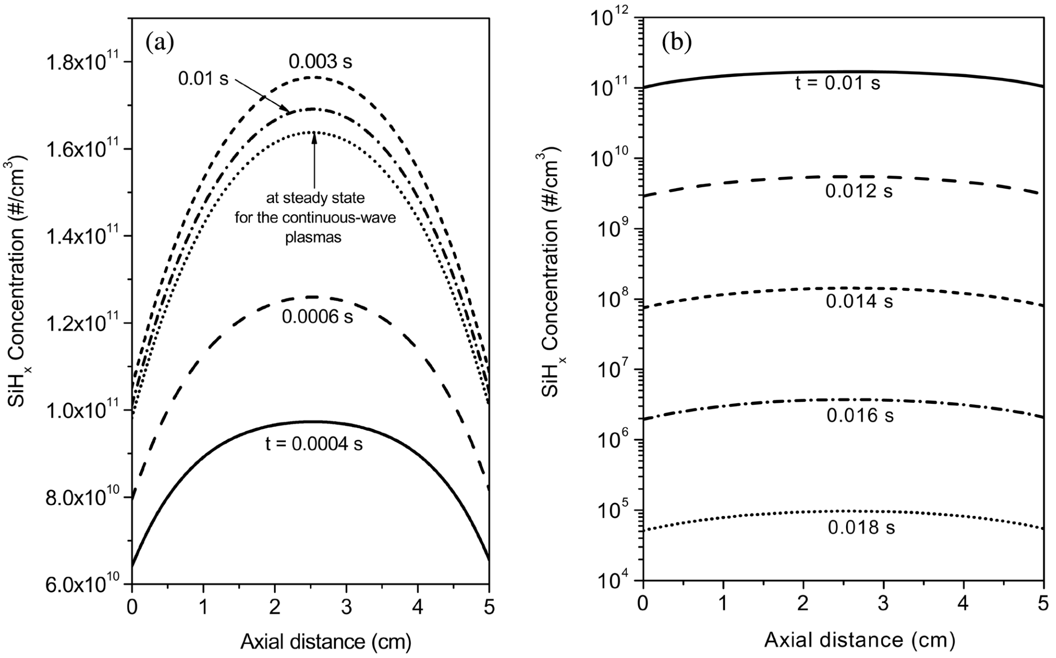

Fig. 3. (a) Evolution of SiH_x concentration profiles along the axial distance for various times during t_{on} (t_{on}=0.01 s and t_{off}=0.02 s). (b) Evolution of SiH_x concentration profiles along the axial distance for various times during t_{off} (t_{on}=0.01 s and t_{off}=0.02 s).

maximum at t=0.003 s. In this analysis, the SiH_x concentration profile during t_{on} is determined by the balance between the diffusion of SiH_x and plasma reactions related to SiH_x. After t=0.003 s, the SiH_x concentration decreases with time due to faster disappearance rates of SiH_x (deposition of SiH_x onto the reactor wall and disappearance reaction of SiH_x) than the generation rate of SiH_x. During t_{on}, the SiH_x concentration at the bulk plasmas is higher than that at the electrodes because SiH_x is consumed by the effect of the SiH_x diffusion toward the electrodes. The SiH_x concentration of the pulsed plasmas at t_{on}=0.01 s is higher than that at the steady state for the continuous-wave plasmas by 3%. In Fig. 3(b), during t_{off}, no SiH_x radical is generated any further by the plasma reactions because the electron concentration is zero and the SiH_x concentration decreases quickly with time by the hydrogen adsorption reaction, R_{10}, and by the ef-

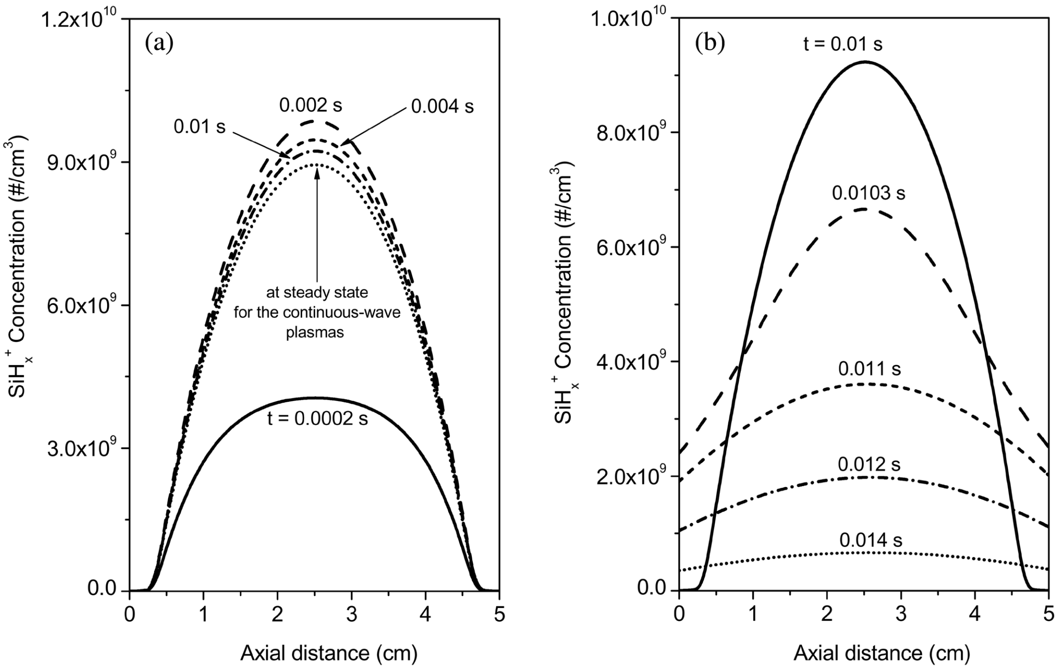

Fig. 4. (a) Evolution of SiH_x^+ concentration profiles along the axial distance for various times during t_{on} (t_{on}=0.01 s and t_{off}=0.02 s). (b) Evolution of SiH_x^+ concentration profiles along the axial distance for various times during t_{off} (t_{on}=0.01 s and t_{off}=0.02 s).

fects of diffusion and fluid convection.

In Figs. 4(a, b), the concentration profiles of SiH_x^+ are shown along the axial distance for various times during t_{on} and t_{off}, respectively. At the start of the plasma discharge, the SiH_x^+ concentration increases quickly by a fast dissociative ionization reaction (R_3) of SiH_4 and reaches the maximum at t=0.002 s, after which its concentration decreases because of faster disappearance reactions (R_8 and R_{11}) of SiH_x^+. The SiH_x^+ concentration for the pulsed plasmas at t=0.01 s is higher than that at the steady state for the continuous-wave plasmas by 3%. During t_{on}, the SiH_x^+ concentrations in the bulk plasmas have sharp peaks on the order of 10^9 #/cm^3, and those in the sheath regions become low on the order of 10^6 #/cm^3 because SiH_x^+ in the sheath regions moves quickly toward the electrodes due to the electrical migration. Just after t_{off}, most of the electrons are consumed rapidly by the ambipolar diffusion with SiH_x^+ and the recombination on the wall, or the electron attachment to the neutrals within 10's μs [Ashida and Lieberman, 1997; Courteille et al., 1996; Fridman et al., 1996; Howling et al., 1994, 1996; Kushner, 1988; Meyyappan, 1996; Midha and Economou, 2000; Ramamurthi and Economou, 2002]. During t_{off}, the SiH_x^+ concentration decreases with time mainly by the neutralization reactions (R_{11}-R_{23}) with negative ions ($Si_nH_x^-$, $n \geq 1$). There is no electric field between the electrodes, and the SiH_x^+ concentrations in the sheath regions increase as SiH_x^+ diffuses from the bulk plasmas to the sheath regions. SiH_x^+ is assumed to be deposited at the electrodes with a sticking coefficient of 0.15 during t_{off} and the SiH_x^+ concentration at the electrode wall after $t \geq 0.011$ s is a little lower than that at the reactor center.

Fig. 5 shows the concentration profiles of $Si_7H_x^-$ along the axial distance during (a) t_{on} and (b) t_{off}. During t_{on}, the concentration of $Si_7H_x^-$ increases with time as a result of the polymerization reactions of negative ions. The negative ions are being pushed toward the bulk plasma region from the sheath regions by an electrostatic repulsion and the $Si_7H_x^-$ concentration becomes nearly zero in the sheath regions and the negative ion concentration profiles show sharp drops in concentration at the sheath boundaries. The negative ion concentration profiles become flat in the bulk plasma region, where the electric field is zero. The model equations for negative ions in this study are not self-consistent because we neglected the governing equation for electrons and the ambipolar diffusion does not affect the evolution of concentration profiles of negative ions. The $Si_7H_x^-$ concentration at the downstream becomes higher than that at the upstream by the effect of fluid convection. The $Si_7H_x^-$ concentration at t=0.01 s of the pulsed plasmas is about 65% of that at the steady state for the continuous-wave plasmas. During t_{off}, the $Si_7H_x^-$ concentration decreases with time due to a disappearance reaction with SiH_x^+ and due to the effects of diffusion and fluid convection. The electric field also disappears in the sheath regions during t_{off}, and the $Si_7H_x^-$ in the bulk plasmas diffuses toward the sheath regions and we can see that some $Si_7H_x^-$ can stay in the sheath regions. Fig. 6 illustrates the concentration profiles of $Si_{13}H_x^-$ along the axial distance during (a) t_{on} and (b) t_{off}. In Figs. 6(a, b), the concentration profiles of $Si_{13}H_x^-$ show the same pattern as $Si_7H_x^-$ in Figs. 5(a, b). The $Si_{13}H_x^-$ concentration at t=0.01 s of the pulsed plasma discharge is lower than that at the steady state for the continuous plasma discharge by about 99%. By using the pulsed plasmas, the growth of polymerized negative ions can be retarded dramatically.

In Fig. 7, the time-averaged SiH_4 concentrations at the reactor center are shown as a function of t_{off} for various t_{on}'s. During t_{off}, the SiH_4 disappearance reactions do not take place and the SiH_4 concentration becomes high and the time-averaged SiH_4 concentration for one cycle of t_{on} and t_{off} increases, as t_{off} increases. During t_{on}, SiH_4 is consumed by the collision with the energetic electrons and the

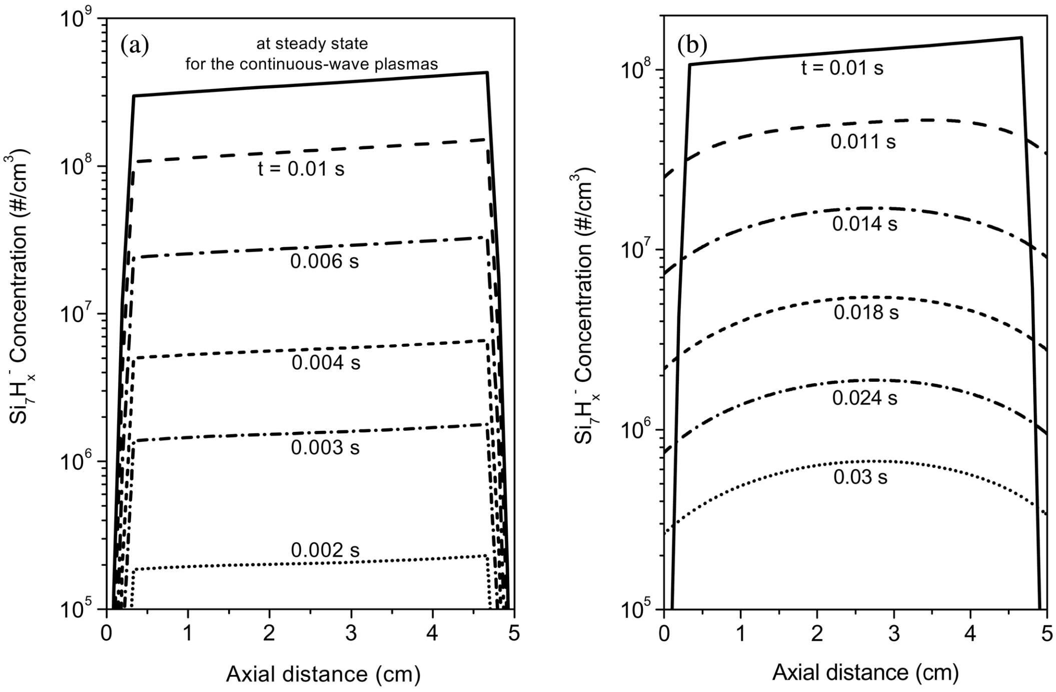

Fig. 5. (a) Evolution of concentration profiles of $Si_7H_x^-$ along the axial distance for various times during t_{on} (t_{on}=0.01 s and t_{off}=0.02 s). (b) Evolution of concentration profiles of $Si_7H_x^-$ along the axial distance for various times during t_{off} (t_{on}=0.01 s and t_{off}=0.02 s).

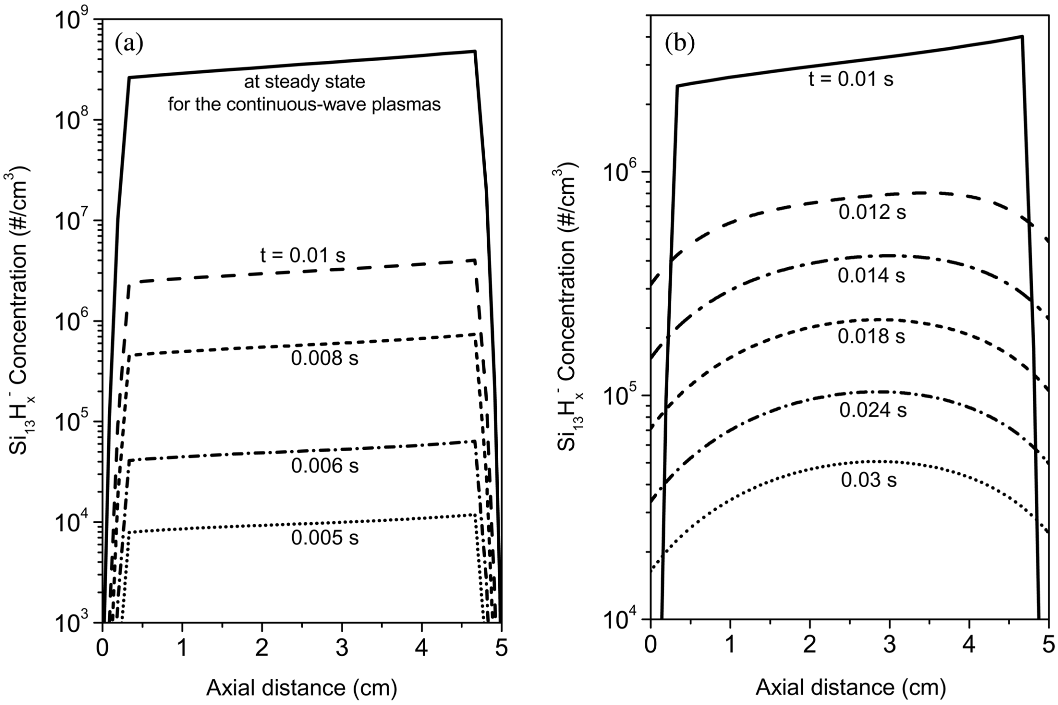

Fig. 6. (a) Evolution of concentration profiles of $Si_{13}H_x^-$ along the axial distance for various times during t_{on} (t_{on}=0.01 s and t_{off}=0.02 s). (b) Evolution of concentration profiles of $Si_{13}H_x^-$ along the axial distance for various times during t_{off} (t_{on}=0.01 s and t_{off}=0.02 s).

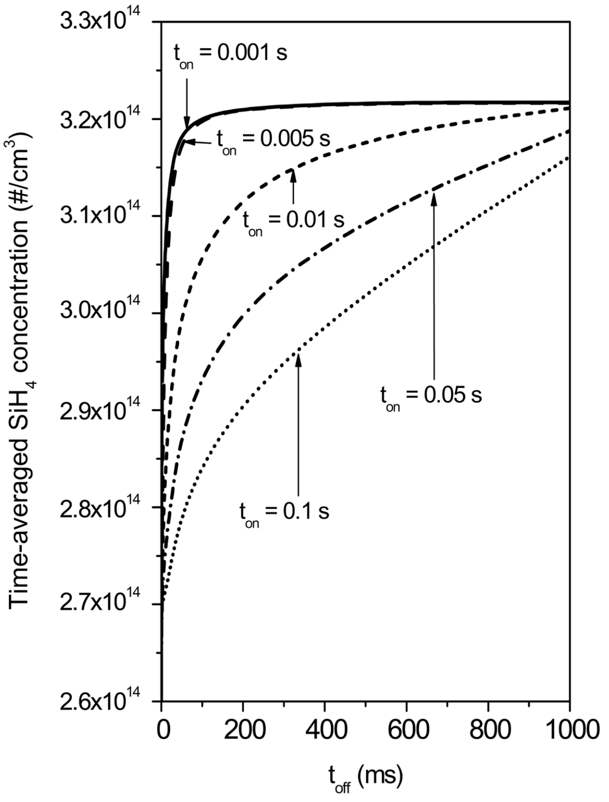

Fig. 7. Time-averaged SiH_4 concentrations at the reactor center as a function of t_{off} for various t_{on}'s.

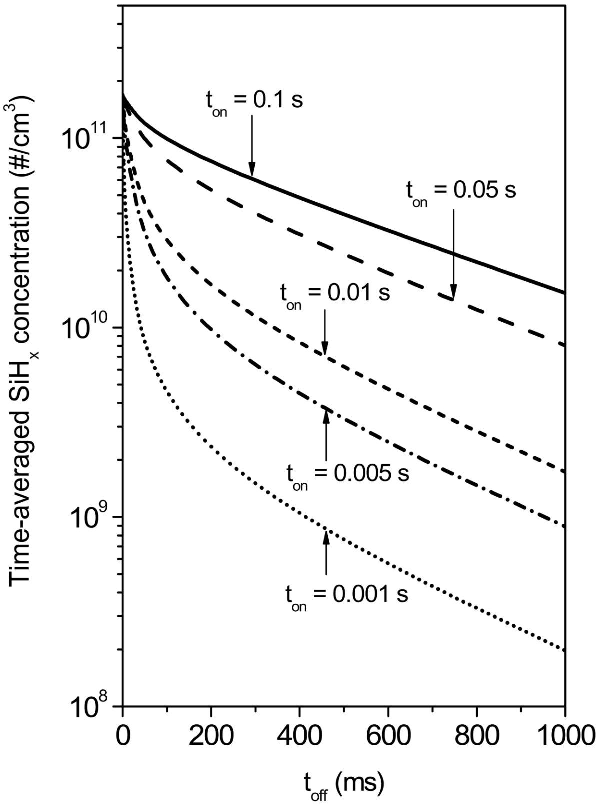

Fig. 8. Time-averaged SiH_x concentrations at the reactor center as a function of t_{off} for various t_{on}'s.

resulting time-averaged SiH_4 concentration decreases with the increase of t_{on}. As t_{off} becomes zero, the time-averaged SiH_4 concentration approaches the SiH_4 concentration at the steady state for the continuous-wave plasmas. The shorter the t_{on} is, the faster the time-

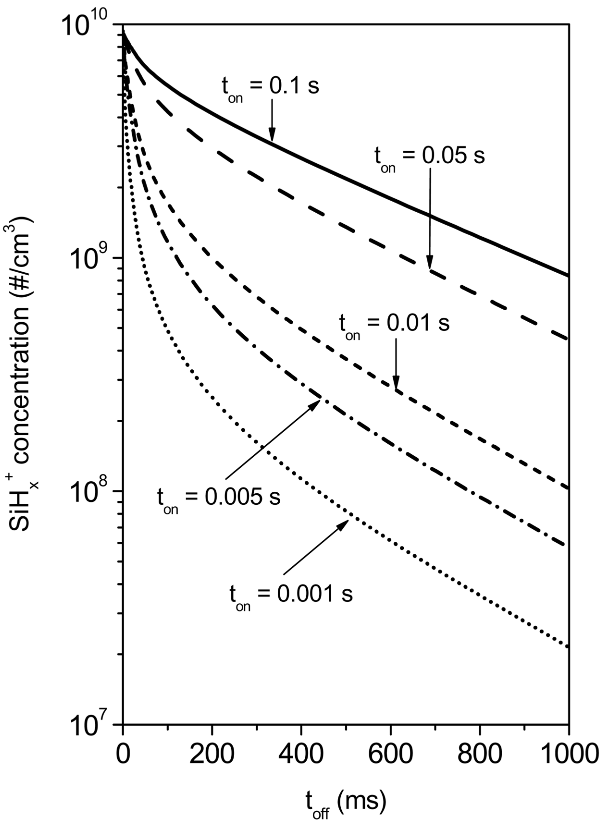

Fig. 9. Time-averaged SiH_x^+ concentrations at the reactor center as a function of t_{off} for various t_{on}'s.

averaged SiH_4 concentration reaches the initial SiH_4 concentration with the decrease of t_{off}. Also, as t_{off} becomes infinite, the time-averaged SiH_4 concentration approaches the initial condition of SiH_4 concentration. Fig. 8 illustrates the time-averaged SiH_x concentrations at the reactor center as a function of t_{off} for various t_{on}'s. During t_{off}, the SiH_x concentration decreases quickly and then becomes zero as shown in Fig. 3(b), and as t_{off} increases, the time-averaged SiH_x concentration decreases. During t_{on}, SiH_x is formed mainly by the SiH_4 dissociation reaction, and as t_{on} increases, the time-averaged SiH_x concentration increases. As t_{off} becomes zero, the time-averaged SiH_x concentration approaches the SiH_x concentration at the steady state. If t_{off} approaches to the infinite level, the averaged SiH_x concentration will become zero.

Fig. 9 shows the time-averaged SiH_x^+ concentrations at the reactor center as a function of t_{off} for various t_{on}'s. As t_{off} increases, the time-averaged SiH_x^+ concentration for the pulsed plasmas decreases because the SiH_x^+ concentration decreases quickly during t_{off}. During t_{on}, positive and negative ions reach steady state concentrations, and the concentrations of negative ions become high. During t_{off}, the SiH_x^+ concentration decreases quickly and becomes zero by fast neutralization reactions with negative ions, and as t_{on} increases, the time-averaged SiH_x^+ concentration increases. In Fig. 10, the time-averaged total concentrations of negative ions ($Si_2H_x^-$~$Si_{13}H_x^-$) at the reactor center are shown as a function of t_{off} for various t_{on}'s. During t_{on}, negative ions are generated, and the time-averaged total concentration of negative ions increases with the increase of t_{on}. During t_{off}, negative ions disappear, and as t_{off} increases, the time-aver-

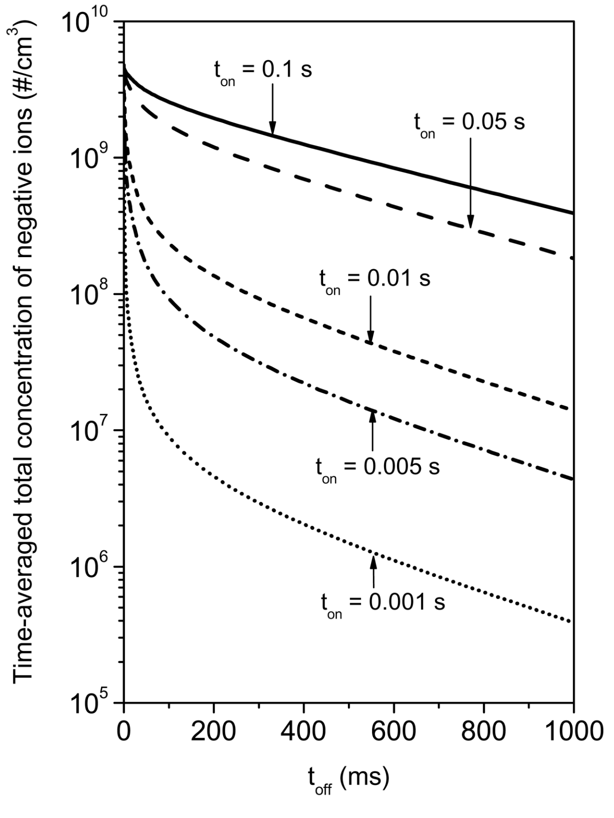

Fig. 10. Time-averaged concentrations of negative ions at the reactor center as a function of t_{off} for various t_{on}'s.

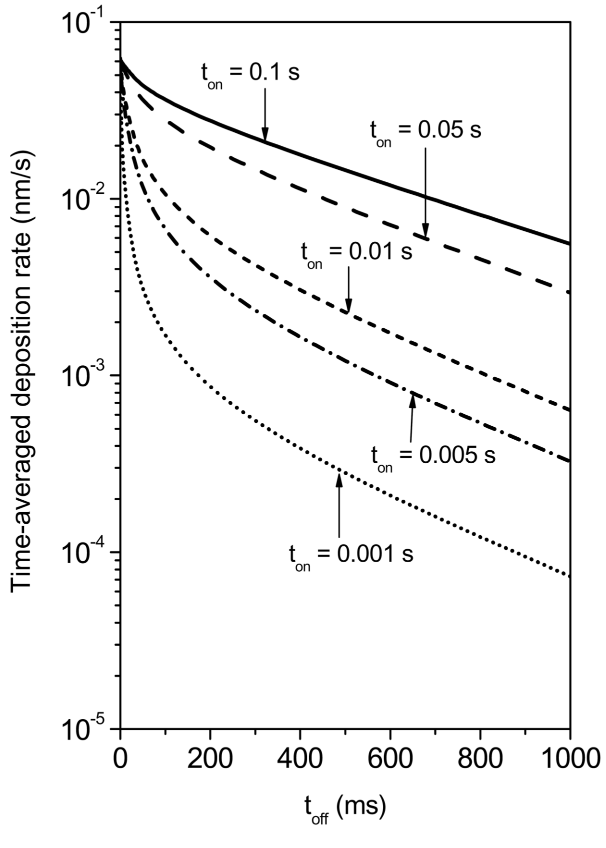

Fig. 11. Time-averaged deposition rates of a-Si : H thin film on the substrate in electrode as a function of t_{off} for various t_{on}'s.

aged total concentration of negative ions decreases. As t_{off} becomes zero, the time-averaged concentration of negative ions approaches the steady state value of the continuous-wave plasmas.

Howling and his colleagues [Howling et al., 1994, 1996] measured the intensities of the radicals and charged species by using the mass spectrometric method and the particles by using the light scattering method in the pulsed plasmas, changing the pulse frequencies (Fig. 3 [Howling et al., 1994, 1996]) and showed that the intensities of the radicals and charged species during t_{on} increase, and during t_{off}, decrease. Watanabe and his co-workers [Fukuzawa et al., 1999; Shiratani et al., 1999] also observed a decrease in particle contamination as the pulse frequency increases (Fig. 9 [Fukuzawa et al., 1999; Shiratani et al., 1999]). Even though we made several assumptions in our modeling, the tendency predicted by the model was in accordance with that observed in the experiments.

In Fig. 11, the time-averaged deposition rates of the a-Si : H thin films on the electrodes are shown as a function of t_{off} for various t_{on}'s. As t_{on} increases or as t_{off} decreases, the time-averaged SiH_x concentration in the reactor increases as shown in Fig. 8 and the growth rate of a-Si : H thin films also increases because of the increase of SiH_x radicals depositing onto the electrodes. Fukuzawa et al. [1999] reported that the deposition rate of the a-Si : H thin films ranges from 0.064 to 0.12 nm/s in the pure SiH_4 plasma reactor without pulse modulation. In this calculation, the film growth rate in the continuous-wave plasmas by the SiH_x radicals is calculated to be about 0.06 nm/s for the same process conditions as in Fukuzawa et al. [1999].

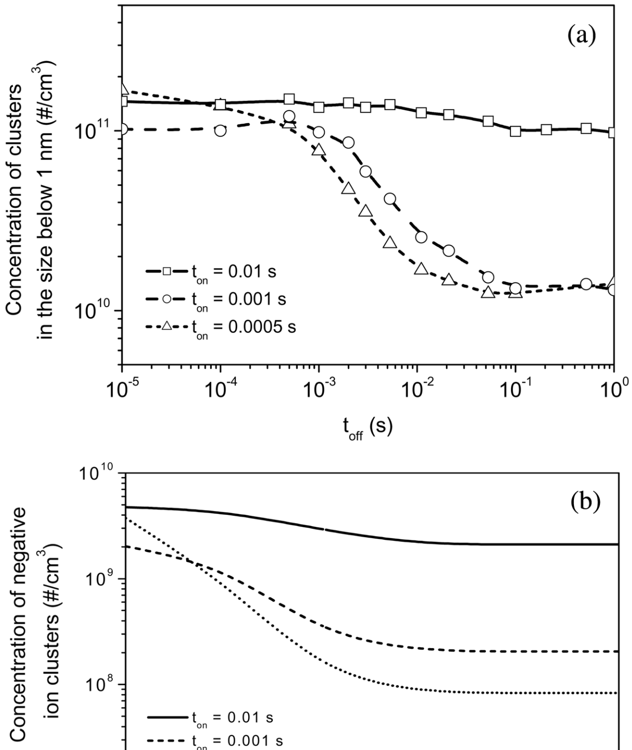

Fig. 12. Concentrations of (a) clusters in the size below 1 nm in experiments [Fukuzawa et al., 1999] and (b) negative ion clusters in this calculation as a function of t_{off} for various t_{on}'s.

The nanosized clusters in the plasma process are considered to be the precursors for the nucleation of particles, and their generation and growth must be suppressed to prepare high-quality thin films [Ashida and Lieberman, 1997; Courteille et al., 1996; Fukuzawa et al., 1999; Howling et al., 1994, 1996; Koga et al., 2002, 2004; Meyyappan, 1996; Shiratani et al., 1999; Watanabe et al., 2002]. Fig. 12 shows (a) the experimental data for the cluster concentrations in the size below 1 nm by Fukuzawa et al. [1999] and (b) the total concentrations of the negative ion clusters ($Si_nH_x^-$, $2 \le n \le 13$) at the reactor center in this calculation for the same process conditions. Both results are in good agreement qualitatively when the summation of t_{on} is exactly 0.1 s for various t_{on}'s. In Figs. 12(a, b), the cluster concentration for t_{off} shorter than 0.0001 s is shown to be nearly constant for various t_{on}'s because the clusters are not removed easily during a short t_{off}. And those results are almost the same as the continuous-wave plasmas. In both results of the experiments and this calculation, the cluster concentration decreases with the increase in t_{off} because the clusters can be removed during t_{off} larger than 0.0001 s. If t_{off} is larger than 0.1 s, the cluster concentration becomes zero at the end of t_{off} and the cluster concentration at the end of each t_{on} becomes almost the same as the change of t_{off}. More clusters are generated with the increase of t_{on}, and the larger the t_{on} is, the higher the cluster concentration is. We used the electron collision rate constants proposed by Kushner which might be different from the experimental conditions [Kushner, 1988]. Also, Fukuzawa et al. [1999] measured the cluster concentration in the size range below 1 nm (which is equivalent to the Si number of about 24), but our model results are for negative ion clusters of $Si_2H_x^-$~$Si_{13}H_x^-$, which might be the reason that our model results of negative ion clusters are less than the experimental results in Fukuzawa et al. [1999]. The negatively charged clusters are hard to arrive at the deposition films during the plasma-on, but some of them can deposit on the films during the plasma-off because there is no electric field between the electrodes. Also, by the neutralization reactions, the negatively charged clusters can become neutral clusters which can be easily deposited onto the thin films even during the plasma-on. Fig. 12 shows that the pulsed plasma process can be an efficient method to suppress the generation and growth of negative ion clusters and that high-quality thin films can be successfully prepared by the pulse plasma technique.

CONCLUSIONS

The concentration profiles for several chemical species that might be important for the film growth and particle generation in the SiH_4 plasmas were analyzed theoretically for various t_{on}'s and t_{off}'s in the pulsed plasmas. The effects of plasma chemical reactions, fluid convection, electrical migration, diffusion, and deposition on the electrodes and reactor wall were included in the model equations for chemical species. The evolution of chemical species was investigated for a processing time of 1 s within a reasonable CPU time by including 36 plasma chemical reactions in the pulsed SiH_4 plasmas and by applying a constant concentration and energy of electrons in the plasma reactor.

During t_{on}, the SiH_4 concentration decreases with time by the electron impact dissociation reactions of SiH_4, and during t_{off}, it increases because energetic electrons in the plasmas disappear. During t_{on}, the concentrations of SiH_x and SiH_x^+ increase quickly because of dissociation reactions of SiH_4. During t_{off}, the concentrations of SiH_x and SiH_x^+ decrease mainly due to the reaction with H_2 and the neutralization reactions with negative ions, respectively. During t_{on}, the concentrations of negative ions increase with time due to the polymerization reactions of negative ions, but, during t_{off}, they decrease with time mainly due to the neutralization reactions with SiH_x^+. In the sheath region, during t_{on}, the SiH_x^+ concentration becomes low as a result of fast electrical migration of SiH_x^+, and the concentrations of negative ions become almost zero due to an electrostatic repulsion. During t_{off}, the SiH_x^+ concentration in the sheath regions becomes high because of the SiH_x^+ diffusion from the bulk plasmas to the sheath regions where some negative ions can penetrate.

As t_{on} increases or as t_{off} decreases, the time-averaged SiH_4 concentration decreases and the time-averaged concentrations of SiH_x^+ and negative ions increase. As t_{on} increases or as t_{off} decreases, the time-averaged SiH_x concentration in the plasmas increases and the subsequent growth rate of the a-Si : H films averaged during t_{on} and t_{off} also increases. Our theoretical analysis shows that the pulse-modulated plasma technique can be an efficient method to reduce the polymerized negative ions of higher mass, which are not preferred precursors for high-quality thin films and can also be the sources of particle contamination.

ACKNOWLEDGMENTS

This research (Paper) was performed for the Hydrogen Energy R&D Center, one of the 21st Century Frontier R&D Programs, funded by the Ministry of Science and Technology of Korea.

REFERENCES

Anders, A., "Fundamentals of pulsed plasmas for materials processing," *Surf. Coat. Technol.*, **183**, 301 (2004).

Ashida, S. and Lieberman, M. A., "Spatially averaged (global) model of time modulated high density chlorine plasmas," *Jpn. J. Appl. Phys.*, **36**, 854 (1997).

Chen, F. F., *Introduction to plasma physics and controlled fusion*, 2nd Ed., Plenum press, New York (1984).

Courteille, C., Dorier, J.-L., Hollenstein, Ch., Sansonnens, L. and Howling, A. A., "Partial-depth modulation study of anions and neutrals in low-pressure silane plasmas," *Plasma Sources Sci. Technol.*, **5**, 210 (1996).

Danckwerts, P. V., "Continuous flow systems: Distribution of residence times," *Chem. Eng. Sci.*, **2**, 1 (1953).

Fridman, A. A., Boufendi, L., Hbid, T., Potapkin, B. V. and Bouchoule, A., "Dusty plasma formation: Physics and critical phenomena. theoretical approach," *J. Appl. Phys.*, **79**(3), 1303 (1996).

Fukuzawa, T., Kushima, S., Matsuoka, Y., Shiratani, M. and Watanabe, Y., "Growth of particles in cluster-size range in low pressure and low power SiH_4 RF discharges," *J. Appl. Phys.*, **86**(7), 3543 (1999).

Graves, D. B., "Fluid model simulations of a 13.56-MHz RF discharge: Time and space dependence of rates of electron impact excitation," *Plasma IEEE Trans. on Plasma Sci.*, **62**(1), 88 (1987).

Graves, D. B. and Jensen, K. F., "A continuum model of DC and RF discharge," *Plasma IEEE Trans. on Plasma Sci.*, **ps-14**(2), 78 (1986).

Howling, A. A., Sansonnens, L., Dorier, J.-L. and Hollenstein, Ch., "Time-resolved measurements of highly polymerized negative ions in radio frequency silane plasma deposition experiments," *J. Appl. Phys.*, **75**, 1340 (1994).

Howling, A. A., Courteille, C., Dorier, J.-L., Sansonnens, L. and Hollenstein, Ch., "From molecules to particles in silane plasmas," *Pure & Appl. Chem.*, **68**(5), 1017 (1996).

Itagaki, N., Fukuda, A., Yoshizawa, T., Shindo, M., Ueda, Y. and Kawai, Y., "Plasma parameter measurements and deposition of a-Si : H thin films in pulsed ECR plasma," *Surf. Coat. Technol.*, **131**, 54 (2000).

Kim, K.-S. and Ikegawa, M., "Particle growth and transport in silane plasma chemical vapor deposition," *Plasma Sources Sci. Technol.*, **5**, 311 (1996).

Kim, D.-J. and Kim, K.-S., "Modeling of the evolutions of negative ions in silane plasma chemical vapor deposition for various process conditions," *Jpn. J. Appl. Phys.*, **36**, 4989 (1997).

Kim, D.-J. and Kim, K.-S., "The factors affecting the particle distributions inside the silane PCVD reactor for semiconductor processing," *Aerosol. Sci. Technol.*, **32**, 293 (2000).

Kim, K.-S. and Kim, D.-J., "Modeling of rapid particle growth by coagulation in silane plasma reactor," *J. Appl. Phys.*, **87**(6), 2691 (2000).

Kim, D.-J. and Kim, K.-S., "Analysis on nanoparticle growth by coagulation in silane plasma reactor," *AIChE J.*, **48**(11), 2499 (2002a).

Kim, D.-J. and Kim, K.-S., "Rapid growth of particles by coagulation between particles in silane plasma reactor," *Korean J. Chem. Eng.*, **19**, 495 (2002b).

Kim, D.-J., Kim, K.-S. and Zhao, Q.-Q., "Production of monodisperse nanoparticles and application of discrete-monodisperse model in plasma reactors," *J. Nanoparticle Res.*, **5**, 221 (2003a).

Kim, K.-S., Kim, D.-J., Yoon, J. H., Park, J. Y., Watanabe, Y. and Shiratani, M., "The changes in particle charge distribution during rapid growth of particles in the plasma reactor," *J. Colloid Interface Sci.*, **257**, 195 (2003b).

Kim, D.-J., Lyoo, P. J. and Kim, K.-S., "Analysis on particle contamination in plasma reactor by 2-sized particle growth model," *Korean J. Chem. Eng.*, **20**, 392 (2003c).

Kim, D.-J. and Kim, K.-S., "Quantitative analysis on the growth of negative ions in pulse modulated SiH_4 plasmas," *Ind. Eng. Chem. Res.*, **44**, 7907 (2005).

Kirimura, H., Maeda, H., Murakami, H., Nakahigashi, T., Ohtani, S., Tabata, T., Hayashi, T., Kobayashi, M., Mitsuda, Y., Nakamura, N., Kuwahara, H. and Doi, A., "Study of deposition process in modulated RF silane plasma," *Jpn. J. Appl. Phys.*, **33**, 4389 (1994).

Koga, K., Kaguchi, N., Shiratani, M. and Watanabe, Y., "Correlation between volume fraction of clusters incorporated into a-Si : H films and hydrogen content associated with Si-H_2 bonds in the films," *J. Vac. Sci. Technol.*, **A 22**(4), 1536 (2004).

Koga, K., Kai, M., Shiratani, M., Watanabe, Y. and Shikatani, N., "Cluster-suppressed plasma chemical vapor deposition method for high quality hydrogenated amorphous silicon films," *Jpn. J. Appl. Phys.*, **41**(2), L168 (2002).

Kushner, M. J., "A model for the discharge kinetics and plasma chemistry during plasma enhanced chemical vapor deposition of amorphous silicon," *J. Appl. Phys.*, **63**, 2532 (1988).

Maemura, Y., Fujiyama, H., Takagi, T., Hayashi, R., Futako, W., Kondo,

M. and Matsuda, A., "Particle formation and a-Si : H film deposition in narrow-gap RF plasma CVD," *Thin Solid Films*, **345**, 80 (1999).

Madan, A. and Morrison, S., "High deposition rate amorphous and polycrystalline silicon materials using the pulsed plasma and hot-wire CVD technique," *Solar Energy Mater. Solar Cells*, **55**, 127 (1998).

Madan, A., Morrison, S. and Kuwahara, H., "Progress in high deposition rate amorphous and polycrystalline silicon materials using the pulsed plasma and hot wire CVD deposition technique," *Solar Energy Mater. Solar Cells*, **59**, 51 (1999).

Meyyappan, M., "Analysis of pulse-time modulated high-density discharges," *J. Vac. Sci. Technol.*, **A 14**(4), 2122 (1996).

Midha, V. and Economou, D. J., "Spatio-temporal evolution of a pulsed chlorine discharge," *Plasma Sources Sci. Technol.*, **9**, 256 (2000).

Ramamurthi, B. and Economou, D. J., "Two-dimensional pulsed-plasma simulation of a chlorine discharge," *J. Vac. Sci. Technol.*, **A 20**(2), 467 (2002).

Reid, R. C., Prusniz, J. H. and Sherwood, T. K., *The properties of gases and liquids*, 3rd Ed., McGraw-Hill, New York (1977).

Sato, N. and Tagashira, H., "A hybrid monte/carlo/fluid model of RF plasmas in a SiH_4/H_2 mixture," *IEEE Trans. Plasma Sci.*, **19**(2), 102 (1991).

Shiratani, M., Fukuzawa, T. and Watanabe, Y., "Particle growth kinetics in silane RF discharges," *Jpn. J. Appl. Phys.*, **38**, 4542 (1999).

Watanabe, Y., Shiratani, M. and Koga, K., "Clustering phenomena in low-pressure reactive plasmas. Basis and applications," *Pure Appl. Chem.*, **74**(3), 483 (2002).